Review of nuclear structure calculations in the sd shell for the rp process

W. A. Richter[1,2] *and B. Alex Brown*[3]
[1] iThemba Labs, P.O.Box 722, Somerset West 7129, South Africa [2] Department of Physics, University of the Western Cape, Private Bag X17, Bellville 7535, South Africa, [3] Department of Physics and Astronomy, and National Superconducting Cyclotron Laboratory, Michigan State University, East Lansing, Michigan 48824-1321, USA

Abstract
We have embarked on a systematic study of important astrophysical rp-process rates for sd shell nuclei. Calculations and results for the ^{25}Al(p,γ)^{26}Si, ^{35}Ar(p,γ)^{36}K and ^{29}P(p,γ)^{30}S reactions are discussed, as well as general principles for doing such calculations.

1 Introduction

In explosive stellar environments, such as classical novae and x-ray bursters, thermonuclear radiative capture reactions on unstable nuclei determine the path of nucleosynthesis towards the proton drip line. These processes are often dominated by resonant capture to excited states above the particle-emission threshold and therefore depend critically on the nuclear properties of the levels involved. However, since the required spectroscopic information on proton-rich nuclei is difficult to obtain, one often has to rely on input from theory, or the use of measured properties of the mirror nuclei. For the present work the gamma and proton decay widths have been calculated with several Hamiltonians to find their values and to estimate their theoretical uncertainties. The determination of the level energies to be used for the resonance Q values is discussed in the next section.

2 Procedure for determining energy levels in the final nucleus.

Because of the exponential dependence of the reaction rate on the resonance energy of the final nucleus of the (p,γ) reaction [1], it is imperative to use as accurate energies as possible. Generally there are three different sources for the energies of the final T=1 nucleus that are input into the reaction rate calculations. In order of preference they are: 1) well-established experimental energies 2) in the case of a T=1 nucleus, predicted levels based on the Isobaric Mass Multiplet Equation (IMME) which uses the measured binding energies of the T=1 partners and a theoretical value of the c-coefficient of the IMME [2] 3) level energies calculated with reliable sd-shell two-body interactions, such as USDA and USDB [3].

The method used for 2) is explained in Ref. [15].

According to the IMME

$$B = a + bT_z + cT_z^2, \tag{1}$$

where B is the binding energy of a state. For the three T=1 isobaric states one can then, with $T_z = (N-Z)/2$, substitute $T_z = 1, 0, -1$ alternately, and by rearranging

$$B_p = 2B_o - B_n + 2c \tag{2}$$

for the proton-rich member, where c can be expressed as

$$c = (B_n + B_p - 2B_o)/2. \tag{3}$$

As a specific example, for ^{26}Si one has

$$B_{th}(^{26}\mathrm{Si}) = 2B(^{26}\mathrm{Al}) - B(^{26}\mathrm{Mg}) + 2c_{th}. \tag{4}$$

For the calculation of the b- and c-coefficients of the IMME we use the USDB Hamiltonian [3] for the charge-independent part and add the Coulomb, charge-dependent and charge-asymmetric nuclear Hamiltonian obtained by Ormand and Brown for the sd shell [2]. This composite interaction is called usdb-cdpn in NuShellX [4]. The cd refers to charge-dependent and pn because the calculations are done in the pn formalism. For the nuclei considered in [2], A=18-22 and A=34-39, the 42 b-coefficients were reproduced with an rms deviation of 27 keV and the 26 c-coefficients were reproduced with an rms deviation of 9 keV. There is considerable state-dependence in the c-coefficients (ranging in values from 130 keV to 350 keV) that is nicely reproduced by the calculations (see Fig. 9 in [2]).

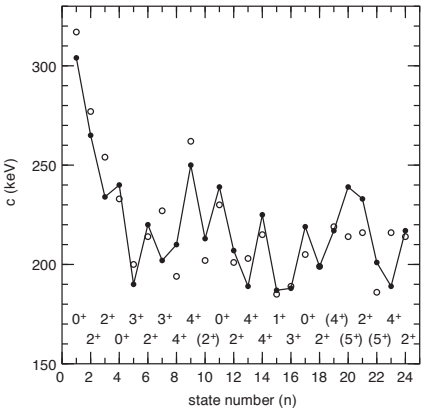

Fig. 1: c-coefficients from the isobaric mass multiplet equation (IMME: $E = a + bT_z + cT_z^2$) versus state number (in order of increasing energy) in ^{26}Si based on experimental energies (closed circles) and energies calculated from USDB (crosses).

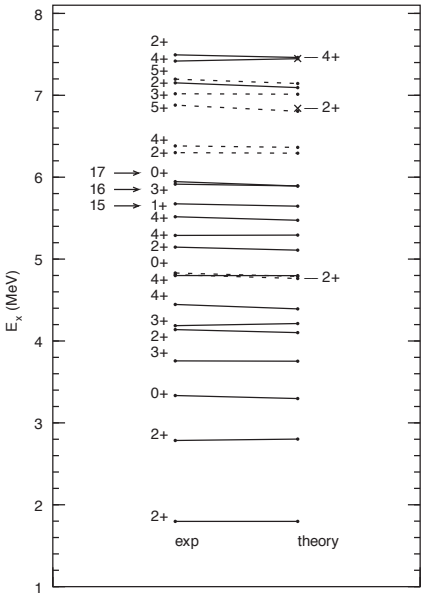

Fig. 2: Adopted experimental excitation energies in ^{26}Si [5] versus predicted energies E_{th} based on experimental binding energies of ^{26}Mg and ^{26}Al and the theoretical c-coefficient (USDB) (Eq. (4)). Dashed lines indicate the uncertain J^π assignments from [5]. The crosses correspond to predicted energies without experimental counterparts.

3 ^{26}Si as the final nucleus

Because many levels in ^{26}Si have uncertainties in terms of energy, spin and parity, a procedure often adopted is to make assignments in ^{26}Si based on known levels in the mirror nucleus ^{26}Mg. We have also made use of experimental information on the levels of excited states in ^{26}Si from Ref. [5]. Using the new sd-shell interactions USDA and USDB [3], as well as the older USD interaction [6], assignments between theory and experiment of corresponding levels in ^{26}Mg levels have been confirmed, and new ones suggested [7]. It has also been shown previously that the new interactions reproduce most observables in the sd shell reliably, and in some cases better than USD [8].

In Fig. (1) values of c from experiment and theory are compared for states in ^{26}Si ordered ac-

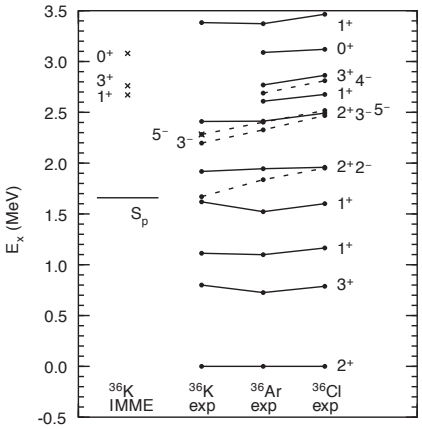

Fig. 3: Experimental energies of the isobaric T=1 triplets for A=36. The energies of ^{36}Ar are relative to the lowest 2^+ T=1 state at 6.611 MeV. Negative parity states are connected by dashed lines. The solid lines connect positive parity states considered to be analogs on the basis of our IMME predictions. The proton separation energy in ^{36}K is shown by the horizontal line on the left-hand side.

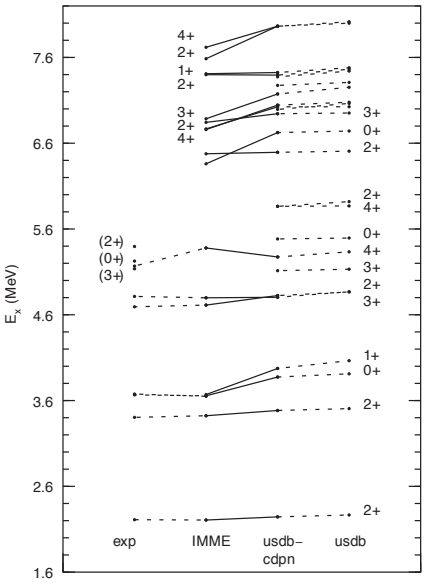

Fig. 4: Experimental excitation energies, predicted IMME-based energies, and usdb-cdpn and usdb energies in ^{30}S.

cording to increasing experimental energy. The experimental values are obtained for states where all three members of the multiplet are known. In general a good correspondence can be seen, the largest deviations being less than 30 keV. There is considerable state dependence with c values ranging from 300 keV (for the 0^+ ground state) down to 180 keV. This IMME method was used in [9] for the T=1 states of the odd-odd nuclei with mass 28, 32 and 36. The agreement with experiment [Fig. (1)] for our even-even case appears to be better than obtained in [9] for the odd-odd cases.

Fig. (2) shows the excitation energies for ^{26}Si obtained from Eq. (2) on the right compared to experiment on the left. The calculated values can then be used as a guide to the correct spin/parity assignments for measured levels in ^{26}Si. Where no levels in ^{26}Si are known, levels can be predicted. Two such levels are indicated by crosses in Fig. (2). The three levels that are just above the proton-decay separation energy of 5.51 MeV and of potential importance for the capture reaction at low temperatures are indicated by the arrows in Fig. (2).

Based on the foregoing discussion, the ^{26}Si energies used for the rate calculations are firstly the established experimental values, then values based on the IMME where data is lacking, and finally values calculated from USDA and USDB when there is insufficient information on the T=1 analog states. The gamma and proton decay widths have been calculated with USDA and USDB.

4 ^{36}K as the final nucleus

Fig. (3) shows the experimental excitation energies of the T=1 analog states for A=36. A number of levels of ^{36}K measured recently by Wrede et al [10] above the proton separation are included, and all other excitation energies are from Ref. [11]. The cross on the 2.282 MeV 5^- state in ^{36}K indicates what this level was associated with the 2^+_3 state by Wrede et al. Our reasons for associating the 2^+_3 level with

the higher state at 2.446 MeV state are discussed in Ref. [12]. The levels labeled ^{36}K IMME are based on Eq. (2) with the experimental binding energies of ^{36}Cl and ^{36}Ar and the theoretical c-coefficient (Eq. (3)). The crosses correspond to predicted energies without experimental counterparts.

In the present case there are two negative parity states, 3^- and 5^- as shown in Fig.(3), close to some of the important resonances, and their contributions should be taken into account. In view of the correspondence between mirror states for A = 36 it would be reasonable to substitute experimental values of the spectroscopic factors and lifetimes from the mirror nucleus ^{36}Cl in cases where a calculation is not feasible. In this way the contributions from these negative parity levels can be taken into account approximately.

5 ^{30}S as the final nucleus

In Fig. (4) experimental energies, energies based on the IMME, and theoretical energies for usdb-cdpn and USDB are shown for ^{30}S. In general the experimental energies and those based on the IMME agree quite well. The experimental energies below 5 MeV are from Ref. [13]. Some new measured energies above 5 MeV from Ref. [14] have also been included (from their Table II). For three of these the energies in the nucleus ^{30}P are uncertain so that IMME values cannot be determined. Where energies could not be predicted from the IMME, values based on usdb-cdpn were used. It is also seen from Fig. (4) that the usdb-cdpn and USDB values do not differ much. Unlabeled theoretical levels (due to space considerations) are, with usdb-cdpn energies given in brackets, 5^+(6.99 MeV), 2^+(7.27 MeV) and 0^+(7.37 MeV).

6 Calculation of the reaction rates

The resonant reaction rate for capture on a nucleus in an initial state i, $N_A < \sigma v >_{\mathrm{res}\,i}$ for isolated narrow resonances is calculated as a sum over all relevant compound nucleus states f above the proton threshold [1]

$$N_A < \sigma v >_{\mathrm{res}\,i} = 1.540 \times 10^{11} (\mu T_9)^{-3/2} \times \sum_f \omega\gamma_{if} \ \mathrm{e}^{-\mathrm{E_{res}}/(kT)} \ \mathrm{cm}^3\,\mathrm{s}^{-1}\mathrm{mole}^{-1}. \quad (5)$$

Here T_9 is the temperature in GigaK, $\mathrm{E}_{res} = \mathrm{E}_f - \mathrm{E}_i$ is the resonance energy in the center of mass system, the resonance strengths in MeV for proton capture are

$$\omega\gamma_{if} = \frac{(2J_f+1)}{(2J_p+1)(2J_i+1)} \frac{\Gamma_{\mathrm{p}\,if}\Gamma_{\gamma f}}{\Gamma_{\mathrm{total}\,f}}. \quad (6)$$

$\Gamma_{\mathrm{total}\,f} = \Gamma_{\mathrm{p}\,if} + \Gamma_{\gamma f}$ is a total width of the resonance level and J_i, J_p and J_f are target, the proton projectile ($J_p = 1/2$), and states in the final nucleus, respectively. Approximations made in calculating the proton width are discussed in Refs. [15], [12].

The total rp reaction rates have been calculated for each of the interactions USD, USDA and USDB for ^{26}Si. The Q values required for ^{26}Si were based on measured energies, and where they were not known values calculated from Eq. (4) were used. Above 8 MeV we used the energies obtained with USDB that includes the addition of about 170 states with $J^\pi \leq 5^+$ up to 14 MeV in excitation energy. Fig. (5) shows the results for the resonance-capture rate obtained using the levels adopted for ^{26}Si (given in Table I, Ref. [15]).

In Fig. (6) the reaction rates leading to ^{36}K are shown. It should be noted that the contribution of the negative parity state 3^- is significant and cannot be neglected, even if it has to based on measured spectroscopic factors and gamma widths of the mirror nucleus ^{36}Cl.

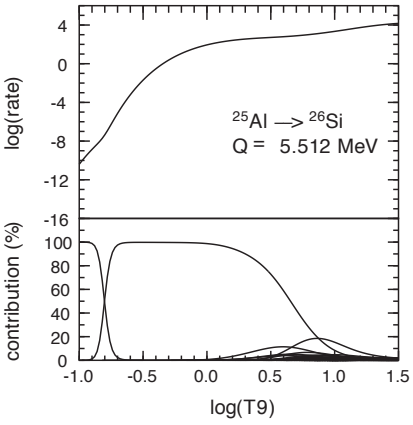

Fig. 5: The total rp reaction rate versus temperature T9 (GigaK) (top panel) and the contribution of each of the final states (lower panel) with USDB. In the lower panel the dominant contribution below log(T9) = −0.8 is from the 1^+ state at 5.675 MeV, and above from the 3^+ state at 5.915 MeV. Γ_γ calculated for ^{26}Si levels.

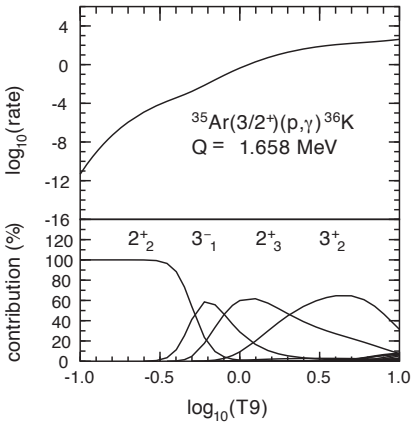

Fig. 6: The total rp reaction rate versus temperature T9 (GigaK) (top panel) and the contribution of each of the final states (lower panel) with usdb-cdpn. Γ_γ was calculated for ^{36}K levels.

In Fig. (7) the results for ^{30}S are shown, indicating that the dominant contributions are from the $3^+(1)$, $2^+(3)$ and $2^+(4)$ states.

7 Uncertainties in the resonant capture reaction rates

A detailed analysis of error sources in the rate calculations has been given in Ref. [15]. A general indication of the variation caused by the use of different interactions can be obtained by comparing the corresponding reaction rates. As an example this is shown in Fig. (8) for the reaction ^{35}Ar(p,γ)^{36}K. Comparisons with the 2010 Evaluation of Monte Carlo-based Thermonuclear Reaction Rates [16] have been made for ^{26}Si and ^{36}K in Refs. [15] and [12] respectively.

8 Conclusions

We have summarized the results of rp reaction rate calculations for three T=1 sd-shell final nuclei. When experimental energies are not available to determine the Q values of the proton capture process, we resorted to the IMME method which is empirically based, except for a contribution from a theoretical c-coefficient. We have demonstrated that a good correspondence between theoretical and experimental values of the c-coefficient for sd-shell nuclei generally exists. The method leads to a reliable prediction of energy levels in the final nucleus provided the energies of the T=1 analog partners are known. The required spectroscopic factors and gamma decay lifetimes for rate calculations were obtained from shell-model calculations using the new sd-shell interactions USDA and USDB (or usda-cdpn and usdb-cdpn) for the charge-independent parts of the interactions. Where some negative parity states occur in the region close to the threshold energy, their contributions to the reaction rate were estimated by using spectroscopic factors and lifetimes of their mirror counterparts. In this way the contributions of such states could be taken into account approximately.

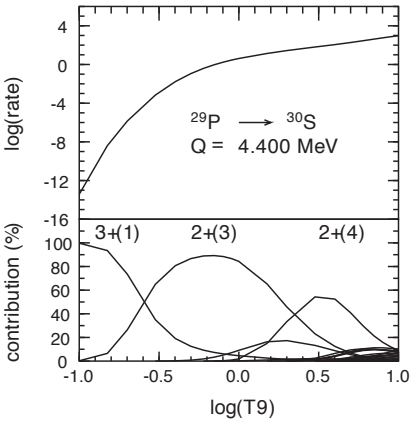

Fig. 7: The total rp reaction rate versus temperature T9 (GigaK) (top panel) and the contribution of each of the final states (lower panel) with usdb-cdpn.

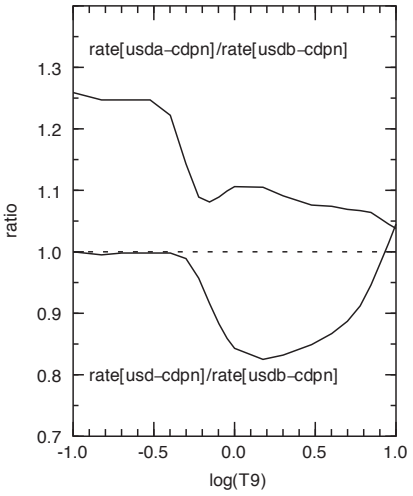

Fig. 8: The total rp reaction rate ratios of usda-cdpn and usd-cdpn versus usdb-cdpn compared.

Acknowledgments This work is partly supported by NSF Grant PHY-1068217 and the National Research Foundation of South Africa under Grant No. 76898.

References

[1] W. A. Fowler and F. Hoyle, Ap. J. Suppl. **9**, 201 (1964).

[2] W. E. Ormand and B. A. Brown, Nucl. Phys. A **491**, 1 (1989).

[3] B. A. Brown and W. A. Richter, Phys. Rev. C **74**, 034315 (2006).

[4] www.nscl.msu.edu/∼brown/resources/resources.html

[5] A. Matic et al., Phys. Rev. C **82**, 025807 (2010).

[6] B. H. Wildenthal, Prog. Part. Nucl. Phys. **11**, 5 (1984).

[7] W. A. Richter and B. A. Brown, Phys. Rev. C **80**, 034301 (2009).

[8] W. A. Richter, S. Mkhize and B. A. Brown, Phys. Rev. C **78**, 064302-1 (2008).

[9] C. Iliadis, P. M. Endt, N. Prantzos and W. J. Thompson, The Astrophysical Jour. **524**, 434 (1999).

[10] C. Wrede, J. A. Clark, C.M. Deibel, T. Faestermann, R. Hartenberger, A. Parikh, H.-F. Wirth, S. Bishop, A. A. Chen, K. Eppinger, B. M. Freeman, R. Krucken, O. Lepyoshkina, G. Rugel and K. Setoodehnia, Phys. Rev. C **82**, 035805 (2010)

[11] P. M. Endt, Nucl. Phys. A **633**, 1 (1998)

[12] W. A Richter and B. A. Brown, Phys. Rev. C **85**, 045806 (2012).

[13] http://www.nndc.bnl.gov/ (2012).

[14] K. Setoodehnia, A. A. Chen, J. Chen, J.A.Clark, C.M. Deibel, S. D. Geraedts, D. Kahl, P. D. Parker, D.Seiler, and C. Wrede, Phys. Rev. C **82**, 022801 (2010)

[15] W. A Richter, B. A. Brown, A. Signoracci and M. Wiescher, Phys. Rev. C **83**, 065803 (2011)

[16] C. Iliadis, R. Longland, A. E. Champagne, A. Coc and R. Fitzgerald, Nucl. Phys. A **841**, 31 (2010).